Published in final edited form as:
J Mol Biol. 2008 January 25; 375(4): 969–978.

Structure of antibody F425-B4e8 in complex with a V3 peptide reveals a new binding mode for HIV-1 neutralization

Christian H. Bell[a], **Ralph Pantophlet**[b], **André Schiefner**[a], **Lisa A. Cavacini**[d,e], **Robyn L. Stanfield**[a], **Dennis R. Burton**[a,b], and **Ian A. Wilson**[a,c,*]

a*Department of Molecular Biology, The Scripps Research Institute, 10550 North Torrey Pines Road, La Jolla, CA 92037, USA*

b*Department of Immunology, The Scripps Research Institute, 10550 North Torrey Pines Road, La Jolla, CA 92037, USA*

c*Skaggs Institute for Chemical Biology, The Scripps Research Institute, 10550 North Torrey Pines Road, La Jolla, CA 92037, USA*

d*Division of Hematology-Oncology, Beth Israel Deaconess Medical Center, Boston, MA 02115, USA*

e*Harvard Medical School, Boston, MA 02115, USA*

SUMMARY

F425-B4e8 (B4e8) is a monoclonal antibody isolated from a human immunodeficiency virus type 1 (HIV-1)-infected individual that recognizes the V3 variable loop on the gp120 subunit of the viral envelope spike. B4e8 neutralizes a subset of HIV-1 primary isolates from subtypes B, C and D, which places this antibody among the very few human anti-V3 antibodies with notable cross-neutralizing activity. Here, the crystal structure of the B4e8 Fab' fragment in complex with a 24-mer V3-peptide (RP142) at 2.8 Å resolution is described. The complex structure reveals that the antibody recognizes a novel V3 loop conformation, featuring a 5-residue α-turn around the conserved GPGRA apex of the β-hairpin loop. In agreement with previous mutagenesis analyses, the Fab' interacts primarily with V3 through side-chain contacts with just two residues, Ile^{P309} and Arg^{P315}, while the remaining contacts are to the main chain. The structure helps explain how B4e8 can tolerate a certain degree of sequence variation within V3 and, hence, is able to neutralize an appreciable number of different HIV-1 isolates.

Keywords

HIV-1; neutralizing antibody; V3; gp120; X-ray crystallography

INTRODUCTION

The envelope spike of the human immunodeficiency virus type 1 (HIV-1) is responsible for viral infectivity by binding to cell surface receptors, thus mediating cell entry[1]. The viral spike is a membrane-anchored, trimeric assembly formed by the non-covalently associated

*Corresponding author, E-mail address of the corresponding author: wilson@scripps.edu

glycoproteins gp120 and gp41. All HIV-1 neutralizing antibodies are directed against these envelope glycoproteins.

Recent crystal structures of broadly neutralizing anti-HIV antibodies have provided insight into the epitope targets of these antibodies and, consequently, strategies to neutralize this constantly evolving virus. One of these epitopes is the membrane proximal region on gp41, which is recognized by human monoclonal antibodies (mAbs) 4E10, the most broadly anti-HIV-1 neutralizing antibody known[2,3], and 2F5[4]. Another suitable epitope for broad neutralization by an antibody is the recessed, but conserved, CD4 binding site on gp120, which is recognized by human mAb b12[5,6]. Structural studies of anti-HIV antibodies have also revealed unique Fab configurations, such as the domain-swapped architecture of mAb 2G12 Fab, that forms a multivalent paratope, specific for oligomannose clusters on gp120[7]. In contrast to these unique broadly neutralizing antibodies, mAbs to the third hypervariable loop (V3) on gp120 neutralize a much smaller range of primary isolates and many tend to be isolate specific[8-11].

The V3 region of gp120 is critical for viral infectivity. V3 mediates the binding to coreceptor molecules on target cells and its sequence determines coreceptor tropism[12-14]. It has been suggested, based on mutagenesis experiments and structural data, that the relatively conserved V3 tip interacts with the extracellular loops of CCR5, thus participating in the gp120 chemokine receptor interaction[15,16]. During cell entry, gp120 undergoes several structural changes, during which V3 may change its conformation, disposition and accessibility. Conformational flexibility in gp120 is supported in part by the crystal structure of unliganded simian immunodeficiency virus (SIV) gp120 core[17,18], which shows significant structural changes in comparison to CD4-bound HIV gp120[19,20] and by an engineered gp120 in complex with mAb b12[6].

A recent crystal structure of HIV-gp120 bound to CD4 and neutralizing antibody X5 revealed the first structural insights into the conformation and relative orientation of the intact V3 loop[15]. The V3 loop comprises approximately 35 residues, linked by a disulfide bond at its base (Cys296-Cys331, HXB2 numbering[21]) and can be subdivided into three parts: the base (residues 296-300 and 326-331), the stem (residues 301-305 and 321-325) and the tip or crown (residues 306-320). In the gp120 structure, the stem region is quite flexible, whereas the base and tip region consist of two antiparallel β-strands that form a β-hairpin loop[15]. The apex of this loop (residues 312-315) is conserved with a GPGR motif in many subtype B viruses and a GPGQ in nearly all non subtype B viruses.

A number of crystal structures of anti-V3 Fabs in complex with V3 peptides have been determined[22-28]. The Fab interactions are mostly centered around the tip region of V3 with its β-turn, with an extended β-structure on its N terminal side; these substructures align well with their corresponding sections in the gp120 structure. V3 peptides have been complexed with murine antibodies 50.1[22,23], 59.1[24,25], 58.2[23], 83.1[26], and human mAbs 2219[27] and 447-52D[28]. All of these V3-structures contain a type II β-turn around the conserved GPGR motif, with the exception of 83.1, that adopts a type I β-turn. In agreement with these crystal structures, the NMR structures of isolated V3-peptides show a high turn propensity around the apex of the hairpin loop[29].

Despite a large repertoire of V3-specific antibodies studied, only a few exhibit neutralization that is not isolate specific. Of these, the two human mAbs 447-52D and 2219 are the best characterized. Human mAb 447-52D utilizes its extended CDR H3 loop to form a mixed β-sheet with the V3-hairpin loop and enlists mainly main-chain interactions to achieve its high affinity and broad specificity[28]. However, it also interacts extensively with the conserved GPGR-crown region, which limits its reactivity to viruses with a GPGR sequence at the V3

tip. Human mAb 2219, on the other hand, binds to the conserved β-structure in the β-hairpin, namely residues P303 to P309, with the crown region, in this case, exposed to solvent. This mode of interaction allows mAb 2219 to recognize V3 peptides with unusual crown sequences[27].

B4e8 is an anti-V3 antibody that initially was thought to recognize an epitope at the base of the V3 loop[30]. However, a recent study[31] re-assessed the epitope designation. It was shown that B4e8 binds to the tip of V3 and that the presence of Ile^{P309}, Arg^{P315} and Phe^{P317} are important for high-affinity binding. In this later study, B4e8 also could neutralize a subset of primary isolates from subtypes B, C and D. In order to investigate the structural basis of this cross-reactivity, we have now determined the crystal structure of B4e8 in complex with the V3 peptide RP142 at 2.8 Å resolution.

RESULTS

Fab' structure

Fab' B4e8 (human, IgG2, κ) was crystallized in complex with the 24-mer,V3-peptide RP142 (Y^{P301}NKRKRIHI^{P309}G^{P312}PGRAFYTTKNIIGC^{P326}) and the structure was determined to 2.8 Å resolution. The heavy and light chains are numbered by the standard Kabat and Wu numbering system[32], whereas the peptide is numbered according to the HXB2 reference sequence[21]. B4e8 is the first human IgG2 that has been structurally characterized (Fig. 1). As expected, the IgG2 C_H1 domain is structurally very similar to human IgG1 C_H1 (rmsd of 0.7 Å for all C_H1 Cα atoms of B4e8 and human IgG1 HIL [PDB ID: 8FAB]); only 6 residues, corresponding to positions 135, 136, 197, 198, 211 and 222, are different.

The CDR loops L1, L2, H1 and H2 fall into canonical classes[33,34] κ2, 1, 1 and 3A, respectively. B4e8 CDR loop L3 shows an insertion after residue 95 which designates it among CDR L3 loops of canonical class κ5. However, the inserted residue is an Asp and not a Pro, as reported for other members of that class[35] and the overall conformation is different from all previously described classes. Thus, the CDR L3 in B4e8 represents a new canonical class for κ-light chains (Fig. 2). The CDR H3 loop is of moderate length (14 residues) compared to other human anti-HIV-1 antibodies with very long H3 loops, such as 2F5 (22), 447-52D (20) or b12 (18). It has a kinked base, as predicted from its sequence[36].

Interestingly, the Fab' is glycosylated at Asn^{H28}, which is part of framework region (FR) 1, with interpretable electron density for the core trisaccharide, $(GlcNAc)_2Man$. A single point mutation in the V_H gene segment creates a glycosylation site by mutation of the conserved Thr^{H28} to Asn^{H28}. However, the sugar does not contact the antigen and, therefore, does not participate in Fab'-peptide interaction. Computer modeling of the antibody structure onto the V3-containing HIV-1 gp120 structure[15] also suggests no likely interaction of the sugar with CD4-bound gp120. Glycosylation of variable antibody domains has been observed previously[37] and at least one other Fab contains a glycosylation site on a conserved framework region[38].

Peptide structure and interactions

The 24-mer V3-peptide RP142 exhibits clear and interpretable electron density in the Fab'-peptide complex for residues P304-P320, except for the Arg^{P304} and Lys^{P305} side chains (Fig. 3). A total of 96 contacts, including four hydrogen bonds and one salt bridge, are formed between B4e8 and RP142 (Table 2). The buried molecular surface area on the Fab' is 447 $Å^2$ and is contributed slightly unequally by the heavy (57%) and light chain (43%), using CDR loops L1 (7%), L3 (36%), H1 (8%), H2 (28%) and H3 (22%). No contacts are made by CDR L2, as frequently observed for haptens and non-protein ligands[39]. The corresponding area on

the peptide is 411 Å^2 and involves all residues from Ile^{P307} to Thr^{P319} with the largest contribution from Arg^{P315} (24%) and Ile^{P309} (21%) (Table 2).

The interaction between the Fab' with the V3 peptide is primarily mediated by limited peptide side-chain, as well as some main-chain, contacts. The side-chain interactions are focussed on only two residues, Ile^{P309} and Arg^{P315}. Together with main-chain contacts along the peptide backbone, these residues participate in 83% of the van der Waals contacts, all hydrogen bonds and the only salt bridge (Fig. 4). Two main-chain hydrogen bonds are formed by Asn^{H108} with Pro^{P313} and Arg^{P315} from the apex of the β-hairpin (Fig. 5). Another main-chain hydrogen bond between the Fab' and the V3-peptide is formed between Leu^{L94} and Phe^{P317}, which further stabilizes their interaction.

The side chain of Arg^{P315} adopts an unusual rotamer that is sandwiched between Tyr^{L32} (~3.7 Å) and Phe^{P317} (~3.7 Å) (Fig. 5). The Arg^{P315} conformation is stabilized by a salt link and a hydrogen bond with Asp^{L92}. The only other major interaction of the Fab' with a V3-peptide side chain involves Ile^{P309}, which is buried in a hydrophobic pocket formed by the CDR H2 loop and Leu^{L94}, and complements the overall surface and charge complementarity between B4e8 and RP142 (Fig. 6). The shape correlation statistic (S_c) of 0.80 is similar to those observed for other Fab-V3-complexes, such as 2219 (PDB-ID: 2B0S, S_c=0.83), 447 52D (1Q1J, 0.77), 59.1 (1ACY, 0.80), 50.1 (1GGI, 0.79), 58.2 (1F58, 0.80) and 83.1 (1NAK, 0.78).

The side chain of His^{P308} is involved in a crystal contact with CDR H2 via a bound Zn^{2+} ion, but does not participate in the B4e8-peptide interaction itself and the conformation of His^{P308} is similar to those observed in other Fab-V3 complexes[15,23,25-28].

Novel V3-conformation

V3 loop structures typically exhibit a β-hairpin conformation with a canonical β-turn for the central GPGR sequence at the tip[15,23,25-28]. The V3 peptide bound to B4e8 adopts this type of overall hairpin conformation, but forms an α-turn around its apex residues Gly^{P312} to Ala^{P316}. α-Turns are defined as five residue turns, with a distance between Cα (*i*) and Cα (*i*+4) of less than 7 Å and a non-helical conformation[40,41]. Hence, the B4e8-peptide structure presented here depicts a novel V3 conformation, which does not exhibit the canonical β-turn for the central GPGR sequence at the tip. The extended N-terminal region of the peptide (R^{P304}KRIHI^{P309}) is structurally very similar to other Fab-bound V3-peptides or the gp120 structure, as reflected by the similarity of their dihedral angles. The subsequent loop region (G^{P312}PGRA^{P316}) is twisted, when compared to the 447-52D, 59.1 or the gp120 structures. A similar twist was observed in the 2219 structure, which resulted from a difference in the ψ angle of Ile^{P309}. Indeed, in the B4e8 structure, this angle is equivalently perturbed, resulting in conformational similarity of the V3-peptides bound to B4e8 and 2219, but only up to Pro^{P313}, as evident by their similar dihedral angles (Table 3, Fig.7).

At the tip of the loop, residues Gly^{P312} to Ala^{P316} form an α-turn with a hydrogen bond between Gly^{P312} N (*i*) and Ala^{P316} O (*i*+4). A search of the PDB revealed that at least 45 other structures have α-turns with similar dihedral angles. In all V3 structures reported previously, the structural motif around residues Gly^{P312} to Arg^{P315} displays a type II or, in the case of 83.1, a type I β-turn. Thus, the structure of the B4e8-peptide complex depicts a novel V3 conformation that highlights its conformational flexibility. The change of the four-residue β-turn (G^{P312}PGR^{P315}) to a five-residue α-turn conformation spanning Gly^{P312} to Ala^{P316} is a result of the structural insertion of Arg^{P315} into the apex of the loop. The much wider turn at the loop tip renders the Arg^{P315} side chain unusually accessible and close to the CDR L1 and L3 loops, thus permitting numerous interactions with the Fab' (Fig. 5).

As a result of the insertion of Arg^{P315} into the turn region of the β-hairpin conformation, the hydrogen bond pattern of the peptide is shifted by one residue compared to other V3-structures. This register shift is most obvious in a comparison of the peptides bound to B4e8 and human mAb 2219, where the position of the side chains of residues P316 to P318 in B4e8 is almost identical to residues P315 to P317 in 2219 (Fig. 7). In the context of gp120, careful inspection of the V3-containing gp120 structure[15] suggests that the shift of the hydrogen bond pattern can be accommodated by the flexible stem region without major rearrangements of the conserved V3-base.

The one residue shift is a result of a 180° rotation of the ψ-angle of the central Gly^{P314} compared to the 2219 or the V3-containing gp120 core structure (Table 3). As a consequence, all subsequent residues are correspondingly rotated, which allows the insertion of Arg^{P315} into the turn region and the aforementioned displacement in hydrogen bonding pattern. A shift of the β-strands with respect to each other has been observed before in the NMR structure of a V3-peptide derived from the HIV strain IIIB in complex with mAb 447-52D[42]. Furthermore the B4e8 structure an additional interstrand hydrogen bond is found between Lys^{P305} and Thr^{P320}, thus extending each β-strand by two residues, compared to the 2219 complex structure[27].

DISCUSSION

Human mAb B4e8 neutralizes a subset of viruses from HIV-1 subtypes B, C and D[31]. The structure of the B4e8-Fab' in complex with the peptide RP142, which comprises the V3-loop sequence of the MN isolate HIV-1 envelope gp120, was determined to provide structural insight into the cross-reactivity of B4e8. Our results illustrate how this antibody can tolerate sequence variability at certain positions within V3. A previous study[31] showed that the interaction of mAb B4e8 with the V3 loop is critically affected by mutating Ile^{P309}, Arg^{P315} or Phe^{P317}. Ile^{P309} is buried in a hydrophobic pocket formed by CDR H2 and Leu^{L94}. As a consequence, position 309 in V3 requires small, hydrophobic residues, such as Ile, Leu and Val, for high affinity antibody binding. Interestingly, the most commonly found residues at this position in V3 loops are Ile, Leu, Phe and Met[43]. Computer modeling suggests that the side chains of Phe and Met would be too large to be accommodated by the Fab' hydrophobic pocket, in good agreement with the inability of B4e8 to neutralize subtype B viruses with a Met at position 309[31].

The majority of interactions between B4e8 and V3 involve Arg^{P315}. An Ala or Gln substitution at this position severely reduces the affinity of B4e8 for V3[31]. Computer modeling of the Arg to Gln mutation suggests that Gln could maintain the hydrogen bond with Asp^{L92}, although most of the van der Waals contacts with Tyr^{L32} and the salt bridge with Asp^{L92} would not be formed. Interestingly, B4e8 was able to neutralize one subtype C and one subtype D virus, albeit at high concentrations, both of which have Gln at this position[31]. We speculate that the ability of F425-Be48 to neutralize the two non-B viruses in the previous study could be due to an optimal presentation of the V3 loop on these viruses to the antibody, thus, compensating for the fewer number of contacts with Gln^{315}. The reason for the inability of B4e8 to neutralize the other viruses is not fully clear. It is certainly possible that the V3 region on these other viruses is not accessible to B4e8. Further studies will be required to adequately address this issue.

The third residue critical for B4e8 binding is Phe^{P317}. Its side chain participates only weakly in the interaction between Fab' and peptide (Table 2). However, it is in close contact (~3.7 Å) with the guanidino side chain of Arg^{P315} and presumably stabilizes the unusual rotamer conformation of Arg^{P315} by diminishing its structural flexibility (Fig. 6). Therefore, Phe^{P317} participates in positioning Arg^{P315} for optimal recognition by B4e8.

The V3 conformation in the complex-structure with B4e8 has not been observed previously and illustrates the conformational flexibility inherent in certain regions of V3. Despite significant structural homology among all eight V3 crystal structures determined so far, it has become apparent that small changes can lead to variable accessibility for the same sets of residues, as well as differential accessibility for different regions of the V3 loop. This scenario can limit and vary the exposure of conserved residues for recognition by potential neutralizing antibodies.

Nevertheless, aside from B4e8, two other moderately broadly neutralizing antibodies, namely 447-52D and 2219, have been elicited against the V3 loop and have been structurally characterized. These three structures reveal three quite distinct modes of recognition for a plethora of viral isolates, through main-chain interactions between the CDR H3 loop and the N-sterminal part of V3 (447-52D), by binding to a conserved face of V3 that allows variation in the tip (2219), or by recognition of a unique V3 conformation (B4e8).

In summary, these results add substantially towards a complete understanding of the V3 loop as a potential target for neutralization of HIV-1. In the future, additional neutralizing and non-neutralizing V3 antibody structures will provide further insights into how such structural information can be utilized with regard to rational design of V3-based antigens that may elicit cross-reactive immune responses.

MATERIALS AND METHODS

Fab' production and purification

Human IgG B4e8 (IgG2, κ) was prepared as previously reported[30]. Briefly, mononuclear splenocytes of an HIV-1 infected patient were transformed with Epstein Barr virus for 48 h and fused with HMMA human myeloma cells[44]. Hybridomas were selected on their specific reactivity with HIV-infected cells and their ability to capture a relatively high degree of virions in a virus capture assay[30]. Fab' fragments were prepared by cleavage of B4e8 IgG with 1 % pepsin (w/w) for 1 h at 37°C and subsequent reduction with 1.5 mM dithiothreitol for 4 h at 37°C. The Fab' fragment was then purified by size exclusion chromatography in 10 mM Hepes, pH 7.5 and 150 mM NaCl on a Superdex 200 16/60 column.

Crystallization and data collection

The peptide (YNKRKRIHIGPGRAFYTTKNIIGC) used for co-crystallization was previously termed RP142[45]. The B4e8-peptide complex was prepared by mixing the Fab' and the peptide in a 1:5 molar ratio in 10 mM Hepes, pH 7.5 and 150 mM NaCl and incubating overnight at 4°C. Crystals were grown by sitting drop vapor diffusion. Drops containing 0.3 μl B4e8-peptide complex (9 mg/ml) and 0.3 μl well solution were equilibrated against 0.5 ml well solution of 16 % polyethylene glycol (PEG) 8000, 100 mM MES, pH 6.0, and 150 mM zinc acetate. Crystals appeared after two days and reached their final size of 80 × 20 × 5 μm^3 after one week. Data to 2.80 Å resolution were collected at the Stanford Synchrotron Radiation Laboratory (SSRL) beamline 11-1, with an overall R_{sym} of 10.2 %, due to low overall I/σ, and a completeness of 99.0 %. Data were processed with the HKL2000 package[46] (see Table 1 for complete data collection and refinement statistics).

The crystals were indexed in monoclinic space group P2 with unit cell dimensions a=82.9Å, b=39.9Å and c=98.0Å with β-=108.5° and one B4e8-peptide complex in the asymmetric unit. The Matthews' coefficient[47] was 3.0 $Å^3$/Da corresponding to a solvent content of ~59%.

Structure determination, refinement and analysis

The structure was determined by molecular replacement using MERLOT[48] and Phaser[49]. The former program was used to search a library of 243 Fab molecules to obtain the best fitting variable domain. Phaser was used for the consecutive rotation and translation of the models. The Fab' constant and variable domains were treated as separate search models using equivalent fragments from PDB entries 1N0X[50] and 1JHL[51], respectively. After initial rigid body and restrained refinement, R_{cryst} dropped to 35.4 % with an R_{free} of 42.7 %. Several cycles of model building and restrained refinement, with maintenance of the same test set of 5 % of reflections throughout, were carried out using Coot[52] and Refmac553, respectively. No interpretable density was found for residues H128 to H136 and residues H196 to H199; therefore, these residues were not built into the model. Final refinement statistics are outlined in Table 1. The quality of the structure was analyzed using the programs MolProbity[54] and WHATIF[55]. Buried molecular surface areas were calculated with the program MS[56] using a probe radius of 1.7 Å and standard van der Waals radii[57]. Shape correlation statistics (S_c) were calculated with CCP4 Sc, version 2.0[58]. Hydrogen bonds were evaluated with the HBPLUS[59] and van der Waals contacts were analyzed with Contacsym[60,61]. The elbow angle was determined to be 134° using RBOW[62].

Protein Data Bank accession code

The atomic coordinates and structure factors have been deposited with the RCSB Protein Data Bank and are available under accession code 2QSC.

Supplementary Material

Refer to Web version on PubMed Central for supplementary material.

ACKNOWLEDGEMENT

We thank D. Shore and P. Verdino for helpful discussions and comments on the manuscript, H. Doherty for IgG purification, R. Aguilar-Sino and S. Ferguson for help with antibody fragmentation and SSRL Beamline 11-1 for synchrotron beamtime.

We gratefully acknowledge support by NIH grants GM46192 (I.A.W. and R.L.S.), AI33292 (D.R.B.), AI63986 (L.A.C.), the International AIDS Vaccine Initiative (IAVI) Neutralizing Antibody Consortium (I.A.W., D.R.B.), a Skaggs predoctoral fellowship (C.H.B.) and a German Academic Exchange Service (DAAD) fellowship (C.H.B.).

This is manuscript 19052-MB from The Scripps Research Institute.

REFERENCES

1. Wyatt R, Sodroski J. The HIV-1 envelope glycoproteins: fusogens, antigens, and immunogens. Science 1998;280:1884–1888. [PubMed: 9632381]
2. Cardoso RM, Zwick MB, Stanfield RL, Kunert R, Binley JM, Katinger H, Burton DR, Wilson IA. Broadly neutralizing anti-HIV antibody 4E10 recognizes a helical conformation of a highly conserved fusion-associated motif in gp41. Immunity 2005;22:163–173. [PubMed: 15723805]
3. Zwick MB, Jensen R, Church S, Wang M, Stiegler G, Kunert R, Katinger H, Burton DR. Anti-human immunodeficiency virus type 1 (HIV-1) antibodies 2F5 and 4E10 require surprisingly few crucial residues in the membrane-proximal external region of glycoprotein gp41 to neutralize HIV-1. J. Virol 2005;79:1252–1261. [PubMed: 15613352]
4. Ofek G, Tang M, Sambor A, Katinger H, Mascola JR, Wyatt R, Kwong PD. Structure and mechanistic analysis of the anti-human immunodeficiency virus type 1 antibody 2F5 in complex with its gp41 epitope. J. Virol 2004;78:10724–10737. [PubMed: 15367639]
5. Saphire EO, Parren PW, Pantophlet R, Zwick MB, Morris GM, Rudd PM, Dwek RA, Stanfield RL, Burton DR, Wilson IA. Crystal structure of a neutralizing human IgG against HIV-1: a template for vaccine design. Science 2001;293:1155–1159. [PubMed: 11498595]

6. Zhou T, Xu L, Dey B, Hessell AJ, Van Ryk D, Xiang SH, Yang X, Zhang MY, Zwick MB, Arthos J, Burton DR, Dimitrov DS, Sodroski J, Wyatt R, Nabel GJ, Kwong PD. Structural definition of a conserved neutralization epitope on HIV-1 gp120. Nature 2007;445:732–737. [PubMed: 17301785]
7. Calarese DA, Scanlan CN, Zwick MB, Deechongkit S, Mimura Y, Kunert R, Zhu P, Wormald MR, Stanfield RL, Roux KH, Kelly JW, Rudd PM, Dwek RA, Katinger H, Burton DR, Wilson IA. Antibody domain exchange is an immunological solution to carbohydrate cluster recognition. Science 2003;300:2065–2071. [PubMed: 12829775]
8. Tugarinov V, Zvi A, Levy R, Hayek Y, Matsushita S, Anglister J. NMR structure of an anti-gp120 antibody complex with a V3 peptide reveals a surface important for co-receptor binding. Structure 2000;8:385–395. [PubMed: 10801487]
9. Binley JM, Wrin T, Korber B, Zwick MB, Wang M, Chappey C, Stiegler G, Kunert R, Zolla-Pazner S, Katinger H, Petropoulos CJ, Burton DR. Comprehensive cross-clade neutralization analysis of a panel of anti-human immunodeficiency virus type 1 monoclonal antibodies. J. Virol 2004;78:13232–13252. [PubMed: 15542675]
10. Gorny MK, Williams C, Volsky B, Revesz K, Cohen S, Polonis VR, Honnen WJ, Kayman SC, Krachmarov C, Pinter A, Zolla-Pazner S. Human monoclonal antibodies specific for conformation-sensitive epitopes of V3 neutralize human immunodeficiency virus type 1 primary isolates from various clades. J. Virol 2002;76:9035–9045. [PubMed: 12186887]
11. Gorny MK, Williams C, Volsky B, Revesz K, Wang XH, Burda S, Kimura T, Konings FA, Nadas A, Anyangwe CA, Nyambi P, Krachmarov C, Pinter A, Zolla-Pazner S. Cross-clade neutralizing activity of human anti-V3 monoclonal antibodies derived from the cells of individuals infected with non-B clades of human immunodeficiency virus type 1. J. Virol 2006;80:6865–6872. [PubMed: 16809292]
12. Basmaciogullari S, Babcock GJ, Van Ryk D, Wojtowicz W, Sodroski J. Identification of conserved and variable structures in the human immunodeficiency virus gp120 glycoprotein of importance for CXCR4 binding. J. Virol 2002;76:10791–10800. [PubMed: 12368322]
13. Hwang SS, Boyle TJ, Lyerly HK, Cullen BR. Identification of the envelope V3 loop as the primary determinant of cell tropism in HIV-1. Science 1991;253:71–74. [PubMed: 1905842]
14. Rizzuto CD, Wyatt R, Hernandez-Ramos N, Sun Y, Kwong PD, Hendrickson WA, Sodroski J. A conserved HIV gp120 glycoprotein structure involved in chemokine receptor binding. Science 1998;280:1949–1953. [PubMed: 9632396]
15. Huang CC, Tang M, Zhang MY, Majeed S, Montabana E, Stanfield RL, Dimitrov DS, Korber B, Sodroski J, Wilson IA, Wyatt R, Kwong PD. Structure of a V3-containing HIV-1 gp120 core. Science 2005;310:1025–1028. [PubMed: 16284180]
16. Dragic T. An overview of the determinants of CCR5 and CXCR4 co-receptor function. J. Gen. Virol 2001;82:1807–1814. [PubMed: 11457985]
17. Chen B, Vogan EM, Gong H, Skehel JJ, Wiley DC, Harrison SC. Structure of an unliganded simian immunodeficiency virus gp120 core. Nature 2005;433:834–841. [PubMed: 15729334]
18. Chen B, Vogan EM, Gong H, Skehel JJ, Wiley DC, Harrison SC. Determining the structure of an unliganded and fully glycosylated SIV gp120 envelope glycoprotein. Structure 2005;13:197–211. [PubMed: 15698564]
19. Kwong PD, Wyatt R, Majeed S, Robinson J, Sweet RW, Sodroski J, Hendrickson WA. Structures of HIV-1 gp120 envelope glycoproteins from laboratory-adapted and primary isolates. Structure 2000;8:1329–1339. [PubMed: 11188697]
20. Kwong PD, Wyatt R, Robinson J, Sweet RW, Sodroski J, Hendrickson WA. Structure of an HIV gp120 envelope glycoprotein in complex with the CD4 receptor and a neutralizing human antibody. Nature 1998;393:648–659. [PubMed: 9641677]
21. Ratner L, Fisher A, Jagodzinski LL, Mitsuya H, Liou RS, Gallo RC, Wong-Staal F. Complete nucleotide sequences of functional clones of the AIDS virus. AIDS Res. Hum. Retroviruses 1987;3:57–69. [PubMed: 3040055]
22. Rini JM, Stanfield RL, Stura EA, Salinas PA, Profy AT, Wilson IA. Crystal structure of a human immunodeficiency virus type 1 neutralizing antibody, 50.1, in complex with its V3 loop peptide antigen. Proc. Natl. Acad. Sci. U S A 1993;90:6325–6329. [PubMed: 8327513]

23. Stanfield R, Cabezas E, Satterthwait A, Stura E, Profy A, Wilson I. Dual conformations for the HIV-1 gp120 V3 loop in complexes with different neutralizing Fabs. Structure 1999;7:131–142. [PubMed: 10368281]
24. Ghiara JB, Ferguson DC, Satterthwait AC, Dyson HJ, Wilson IA. Structure-based design of a constrained peptide mimic of the HIV-1 V3 loop neutralization site. J. Mol. Biol 1997;266:31–39. [PubMed: 9054968]
25. Ghiara JB, Stura EA, Stanfield RL, Profy AT, Wilson IA. Crystal structure of the principal neutralization site of HIV-1. Science 1994;264:82–85. [PubMed: 7511253]
26. Stanfield RL, Ghiara JB, Ollmann Saphire E, Profy AT, Wilson IA. Recurring conformation of the human immunodeficiency virus type 1 gp120 V3 loop. Virology 2003;315:159–173. [PubMed: 14592768]
27. Stanfield RL, Gorny MK, Zolla-Pazner S, Wilson IA. Crystal structures of human immunodeficiency virus type 1 (HIV-1) neutralizing antibody 2219 in complex with three different V3 peptides reveal a new binding mode for HIV-1 cross-reactivity. J. Virol 2006;80:6093–6105. [PubMed: 16731948]
28. Stanfield RL, Gorny MK, Williams C, Zolla-Pazner S, Wilson IA. Structural rationale for the broad neutralization of HIV-1 by human monoclonal antibody 447-52D. Structure 2004;12:193–204. [PubMed: 14962380]
29. Galanakis PA, Spyroulias GA, Rizos A, Samolis P, Krambovitis E. Conformational properties of HIV-1 gp120/V3 immunogenic domains. Curr. Med. Chem 2005;12:1551–1568. [PubMed: 15974987]
30. Cavacini L, Duval M, Song L, Sangster R, Xiang SH, Sodroski J, Posner M. Conformational changes in env oligomer induced by an antibody dependent on the V3 loop base. AIDS 2003;17:685–689. [PubMed: 12646791]
31. Pantophlet R, Aguilar-Sino RO, Wrin T, Cavacini LA, Burton DR. Analysis of the neutralization breadth of the anti-V3 antibody F425-B4e8 and re-assessment of its epitope fine specificity by scanning mutagenesis. Virology 2007;364:441–453. [PubMed: 17418361]
32. Kabat, EA.; Wu, TT.; Perry, HM.; Gottesman, KS.; Foeller, C. Sequences of Proteins of Immunological Interest. 5th edit.. National Institutes of Health; Bethesda, MD: 1991.
33. Al-Lazikani B, Lesk AM, Chothia C. Standard conformations for the canonical structures of immunoglobulins. J. Mol. Biol 1997;273:927–948. [PubMed: 9367782]
34. Martin AC, Thornton JM. Structural families in loops of homologous proteins: automatic classification, modelling and application to antibodies. J. Mol. Biol 1996;263:800–815. [PubMed: 8947577]
35. Vargas-Madrazo E, Paz-Garcia E. Modifications to canonical structure sequence patterns: Analysis for L1 and L3. Proteins 2002;47:250–254. [PubMed: 11933071]
36. Shirai H, Kidera A, Nakamura H. Structural classification of CDR-H3 in antibodies. FEBS Lett 1996;399:1–8. [PubMed: 8980108]
37. Huang L, Biolsi S, Bales KR, Kuchibhotla U. Impact of variable domain glycosylation on antibody clearance: an LC/MS characterization. Anal. Biochem 2006;349:197–207. [PubMed: 16360109]
38. Qian J, Liu T, Yang L, Daus A, Crowley R, Zhou Q. Structural characterization of N-linked oligosaccharides on monoclonal antibody cetuximab by the combination of orthogonal matrix-assisted laser desorption/ionization hybrid quadrupole-quadrupole time-of-flight tandem mass spectrometry and sequential enzymatic digestion. Anal. Biochem 2007;364:8–18. [PubMed: 17362871]
39. Stanfield RL, Wilson IA. Protein-peptide interactions. Curr. Opin. Struct. Biol 1995;5:103–113. [PubMed: 7773739]
40. Dasgupta B, Pal L, Basu G, Chakrabarti P. Expanded turn conformations: Characterization and sequence-structure correspondence in α-turns with implications in helix folding. Proteins 2004;44:7250–7258.
41. Chou KC. Prediction of tight turns and their types in proteins. Anal. Biochem 2000;286:1–16. [PubMed: 11038267]
42. Rosen O, Chill J, Sharon M, Kessler N, Mester B, Zolla-Pazner S, Anglister J. Induced fit in HIV-neutralizing antibody complexes: evidence for alternative conformations of the gp120 V3 loop and

the molecular basis for broad neutralization. Biochemistry 2005;44:7250–7258. [PubMed: 15882063]

43. Kuiken, CL.; Foley, B.; Hahn, B.; Marx, PA.; McCutchan, F.; Mellors, JW.; Mullins, JI.; Wolinsky, S.; Korber, BE.; Theoretical Biology and Biophysics Group. Human retroviruses and AIDS 1999: a compilation and analysis of nucleic acid and amino acid sequences. Los Alamos National Laboratory; Los Alamos, N. Mex.: 1999.
44. Posner MR, Barrach HJ, Elboim HS, Nivens K, Santos DJ, Chichester CO, Lally EV. The generation of hybridomas secreting human monoclonal antibodies reactive with type II collagen. Hybridoma 1989;8:187–197. [PubMed: 2541068]
45. Javaherian K, Langlois AJ, LaRosa GJ, Profy AT, Bolognesi DP, Herlihy WC, Putney SD, Matthews TJ. Broadly neutralizing antibodies elicited by the hypervariable neutralizing determinant of HIV-1. Science 1990;250:1590–1593. [PubMed: 1703322]
46. Otwinowski Z, Minor W. Processing of X-ray diffraction data collected in oscillation mode. Methods Enzymol 1997;276A:307–326.
47. Matthews BW. Determination of protein molecular weight, hydration, and packing from crystal density. Methods Enzymol 1985;114:176–187. [PubMed: 4079764]
48. Fitzgerald PMD. MERLOT, an integrated package of computer programs for the determination of crystal structures by molecular replacement. J. Appl. Crystallogr 1988;21:273–278.
49. McCoy AJ, Grosse-Kunstleve RW, Storoni LC, Read RJ. Likelihood-enhanced fast translation functions. Acta Crystallogr. Biol. Crystallogr 2005;D61:458–464.
50. Saphire EO, Montero M, Menendez A, van Houten NE, Irving MB, Pantophlet R, Zwick MB, Parren PW, Burton DR, Scott JK, Wilson IA. Structure of a high-affinity “mimotope” peptide bound to HIV-1-neutralizing antibody b12 explains its inability to elicit gp120 cross-reactive antibodies. J. Mol. Biol 2007;369:696–709. [PubMed: 17445828]
51. Chitarra V, Alzari PM, Bentley GA, Bhat TN, Eisele JL, Houdusse A, Lescar J, Souchon H, Poljak RJ. Three-dimensional structure of a heteroclitic antigen-antibody cross-reaction complex. Proc. Natl. Acad. Sci. USA 1993;90:7711–7715. [PubMed: 8356074]
52. Emsley P, Cowtan K. Coot: model-building tools for molecular graphics. Acta Crystallogr. Biol. Crystallogr 2004;D60:2126–2132.
53. Murshudov GN, Vagin AA, Dodson EJ. Refinement of macromolecular structures by the maximum-likelihood method. Acta Crystallogr. Biol. Crystallogr 1997;D53:240–255.
54. Lovell SC, Davis IW, Arendall WB 3rd, de Bakker PI, Word JM, Prisant MG, Richardson JS, Richardson DC. Structure validation by Calpha geometry: phi,psi and Cbeta deviation. Proteins 2003;50:437–450. [PubMed: 12557186]
55. Vriend G. WHAT IF: a molecular modeling and drug design program. J. Mol. Graph 1990;8:52–56. [PubMed: 2268628]
56. Connolly ML. The molecular surface package. J. Mol. Graph 1993;11:139–141. [PubMed: 8347567]
57. Gelin BR, Karplus M. Side-chain torsional potentials: effect of dipeptide, protein, and solvent environment. Biochemistry 1979;18:1256–1268. [PubMed: 427111]
58. Lawrence MC, Colman PM. Shape complementarity at protein/protein interfaces. J. Mol. Biol 1993;234:946–950. [PubMed: 8263940]
59. McDonald IK, Thornton JM. Satisfying hydrogen bonding potential in proteins. J. Mol. Biol 1994;238:777–793. [PubMed: 8182748]
60. Sheriff S, Hendrickson WA, Smith JL. Structure of myohemerythrin in the azidomet state at 1.7/1.3 Á resolution. J. Mol. Biol 1987;197:273–296. [PubMed: 3681996]
61. Sheriff S, Silverton EW, Padlan EA, Cohen GH, Smith-Gill SJ, Finzel BC, Davies DR. Three-dimensional structure of an antibody-antigen complex. Proc. Natl. Acad. Sci. USA 1987;84:8075–8079. [PubMed: 2446316]
62. Stanfield RL, Zemla A, Wilson IA, Rupp B. Antibody elbow angles are influenced by their light chain class. J. Mol. Biol 2006;357:1566–1574. [PubMed: 16497332]
63. Baker NA, Sept D, Joseph S, Holst MJ, McCammon JA. Electrostatics of nanosystems: application to microtubules and the ribosome. Proc. Natl. Acad. Sci. USA 2001;98:10037–10041. [PubMed: 11517324]

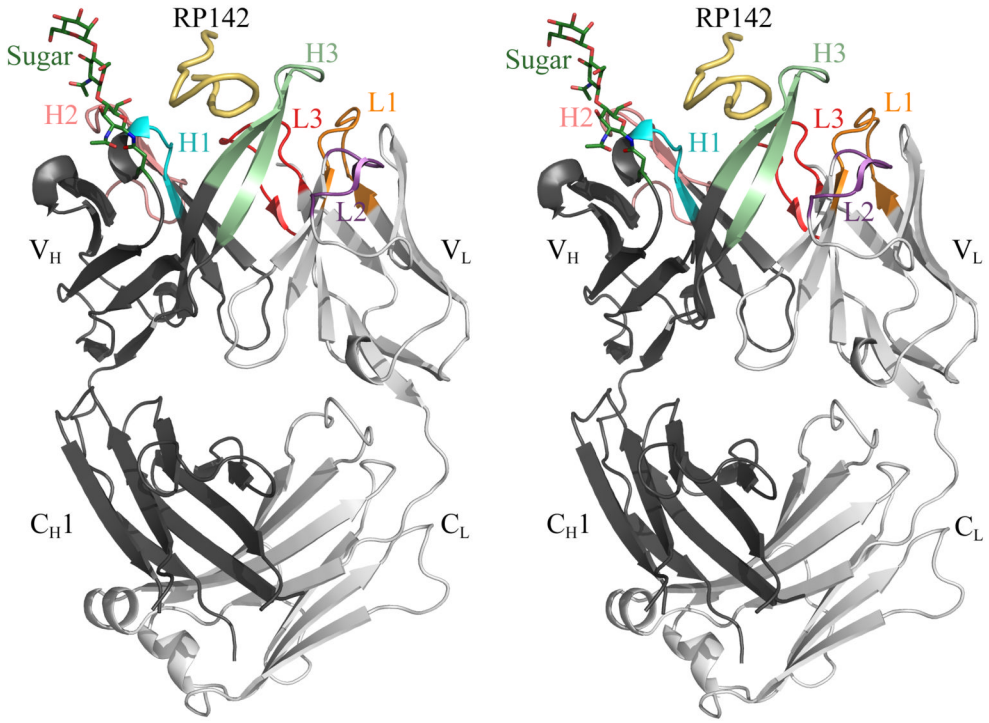

Figure 1.

Crystal structure of the B4e8-RP142 complex. The peptide is colored in yellow and the Fab' heavy and light chains in dark and light gray, respectively; the Fab' CDR loops are colored in orange for L1, purple for L2, red for L3, cyan for H1, salmon for H2 and light green for H3. The sugar and Asn^{H28}, to which it is linked, are shown in stick representation and colored in dark green. Images were produced with Pymol (http://pymol.sourceforge.net/).

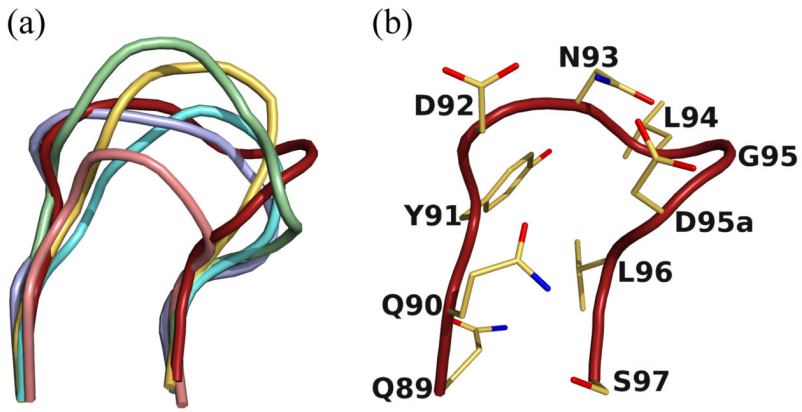

Figure 2.

New canonical class for CDR L3. (a) Comparison of the CDR L3 loop of B4e8 (red) to members of canonical class κ-1 (PDB-code: 1REI, lightblue), κ-2 (2FBJ, yellow), κ-3 (1YQV, aquamarine), κ-4 (1DFB, salmon) and κ-5 (palegreen, 1BAF). (b) The B4e8 kappa chain CDR L3 has an Asp instead of the usual Pro at position 95a and represents a new canonical structure.

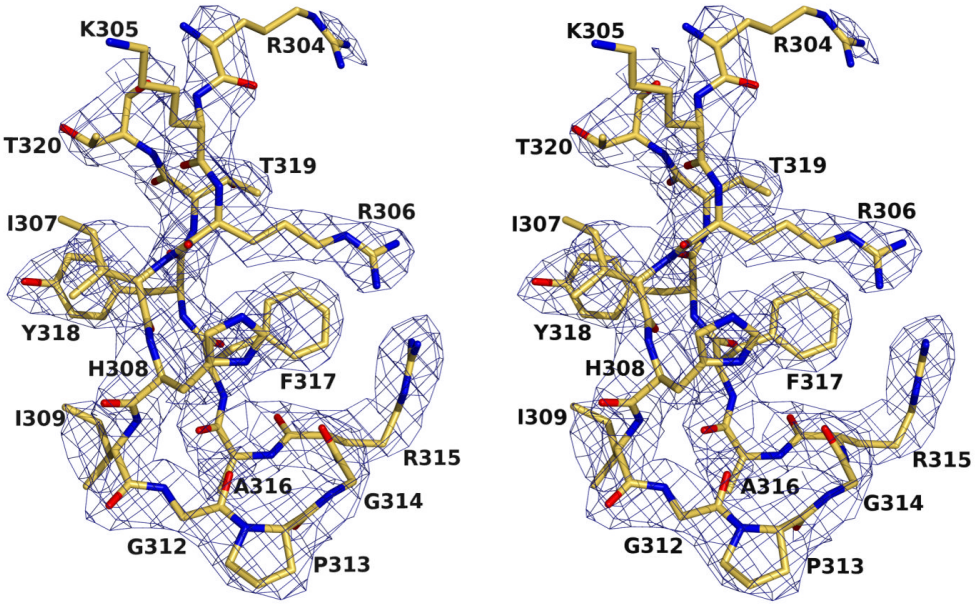

Figure 3.

Electron density ($2F_{obs}$-F_{calc}) for the RP142-peptide in complex with B4e8, contoured at 1.0σ. All residues, except the side chains of Lys^{P305} and Arg^{P304}, are well defined.

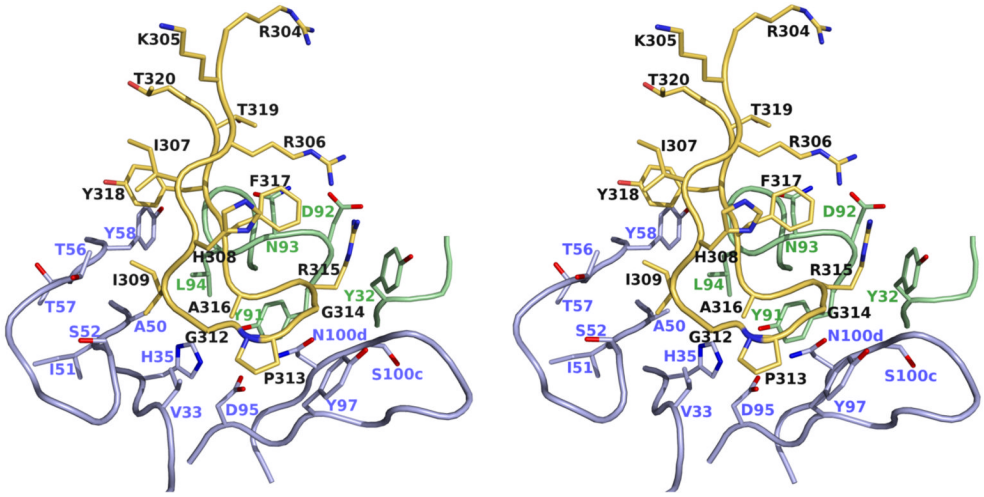

Figure 4.

Specific binding interactions between B4e8 and RP142. Atomic coloring is used for the atoms with the carbon atoms of the peptide colored in yellow, carbon atoms of the heavy chain in light blue and those of the light chain in pale green. Only those residues of the Fab' that make contact to the peptide are shown in stick representation. Residues Gly^{P312} - Ala^{P316} form a five residue α-turn.

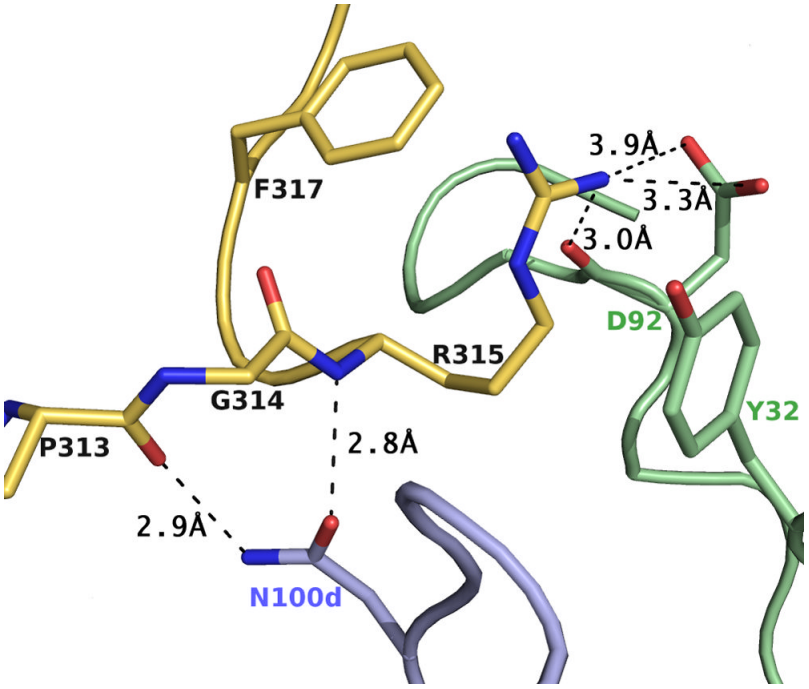

Figure 5.

Detailed view of the exposed Arg^{P315} and its interactions with B4e8. Hydrogen bonds and salt bridges are shown by dashed lines. Color coding is as in Fig. 4. Arg^{P315} is sandwiched between Phe^{P317} and Tyr^{L32} and stabilized by a salt bridge and a hydrogen bond to the side chain and backbone of Asp^{L92}. The unusual α-turn conformation is stabilized by two hydrogen bonds between Asn^{H100d} and the backbone of Arg^{P315} and Pro^{P313}, respectively.

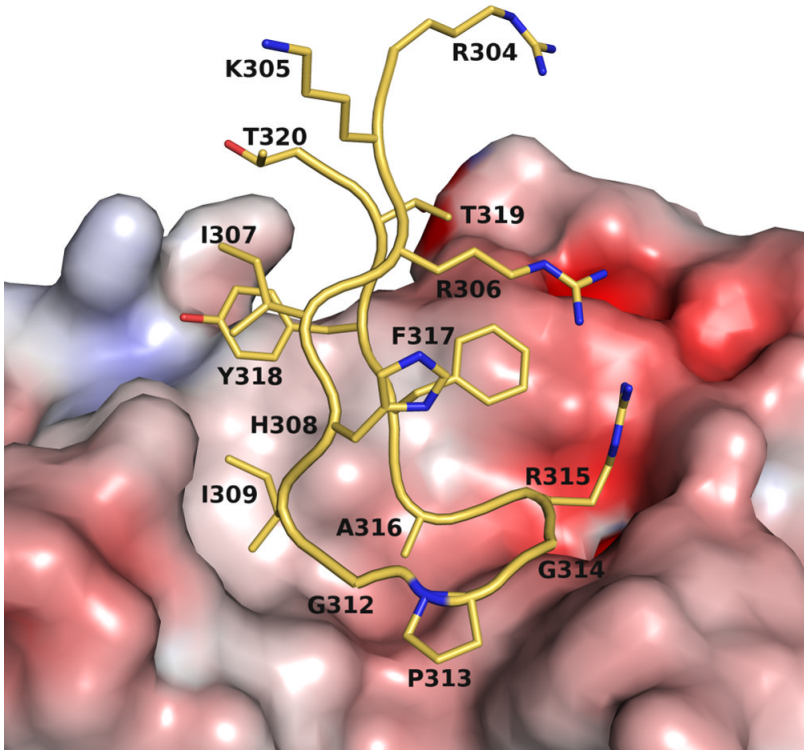

Figure 6.

Molecular surface representation of the antigen-binding pocket colored by electrostatic potential, calculated in APBS[63], and mapped onto the surface with the color code ranging from -10 kT/e (bright red) to +10 kT/e (dark blue). Ile^{P309} is accommodated in a hydrophobic pocket, whereas Arg^{P315} forms a salt bridge with Asp^{L92}.

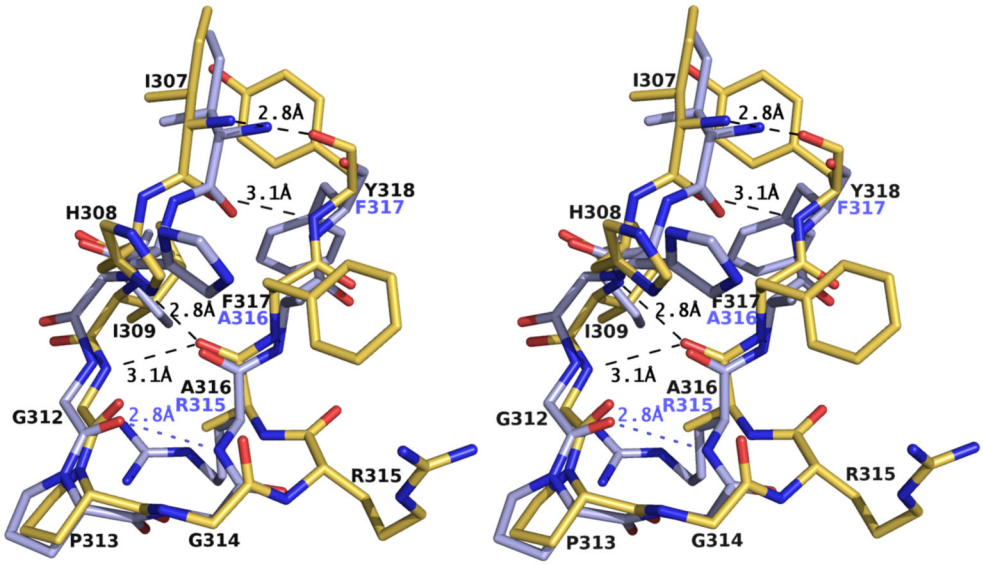

Figure 7.

Comparison of V3-peptides RP142 and MN bound to B4e8 (atomic coloring with carbon atoms in yellow) and 2219 (carbon atoms in light blue), respectively. Identical residues in both peptides are labeled only for B4e8 (black). Identical hydrogen bonds are marked by dashed lines and shown only for B4e8. Due to the conversion from a type II β-turn in 2219 to an α-turn in B4e8, one hydrogen bond in the apex of RP142 is lost in the complex with B4e8. The β-hairpin conformation is maintained by a one-residue shift accompanied by a 180° rotation of Ala^{P316} and all subsequent residues. Residues P304 to P306 and P319 to 320 are omitted for clarity.

Table 1

Data collection and refinement statistics

Data Collection	
Wavelength (Å)	0.979
Resolution (Å)	2.80 (2.87 - 2.80)[a]
Space group, cell	P2
dimension a, b, c (Å), β (°)	82.9, 39.9, 98.0, 108.5
Unique reflections	15,169 (962)
Redundancy	3.7 (3.2)
Completeness (%)	99.0 (94.6)
R_{sym} (%)[b]	10.2 (47.6)
Avg I/σ	12.6 (2.3)
Refinement statistics for all reflections >0.0 σF	
Resolution	50.0 - 2.80
No. of reflections (working)	14,414
No. of reflections (test)	755
R_{cryst} (%)[c]	21.9 (33.0)
R_{free} (%)[d]	26.4 (40.7)
No. of Fab atoms	3,229
No. of peptide atoms	125
No. of water molecules	15
No. of ions (Zn^{2+} / Cl^-)	4 / 4
Overall B value (Å^2):	
Variable domain	49.3
Constant domain	49.4
Peptide	49.4
Water	35.9
Ions	53.6
Sugar	80.0
Wilson B value (Å^2)	60.8
Ramachandran plot (%)[e]	
Favored	96.7
Allowed	3.1
Disallowed[f]	0.2
Root mean square deviations	
Bond length (Å)	0.005
Angle (°)	0.95

[a] Numbers in parenthesis are for the highest resolution shell.

[b] $R_{sym} = \sum hkl \mid I - \langle I \rangle \mid / \sum hkl \mid I \mid$

[c] $R_{cryst} = \sum hkl \mid F_{obs} - F_{calc} \mid / \sum hkl \mid F_{obs} \mid$

[d] R_{free} is the same as R_{cryst} except for 5% of the data excluded from the refinement.

[e] Evaluated with MolProbity [39]

[f] ProH149, which is part of a conserved loop region and in clearly interpretable density.

Table 2

Total hydrogen bond and van der Waals contacts of peptide with B4e8 and buried surface areas of the V3 peptide[a]

Peptide residue	Main[b]	Side[b]	Surface (Å^2)
I^{P307}	0 / 0	0 / 0	8.6
H^{P308}	0 / 0	0 / 0	7.4
I^{P309}	0 / 2	0 / 13	87.9
G^{P312}	0 / 1	0 / 0	9.8
P^{P313}	1 / 5	0 / 4	41.9
G^{P314}	0 / 6	0 / 0	19.5
R^{P315}	1 / 5	1 / 29	96.3
A^{P316}	0 / 6	0 / 2	34.1
F^{P317}	1 / 9	0 / 3	45.7
Y^{P318}	0 / 0	0 / 7	51.7
T^{P319}	0 / 0	0 / 0	10.2

[a] Residues with no buried surface area are not listed.

[b] Shown as: hydrogen bonds / van der Waals contacts

Table 3

Main chain torsion angles (°) bound to Fabs B4e8, 2219 and the V3-region in the gp120 core

Peptide residue	Angle	B4e8	2219MN	gp120	Average deviation[a]
R^{P304}	ϕ		-109	-108	1
	ψ	51	24	148	49
K^{P305}	ϕ	-81	-75	-124	20
	ψ	151	-32	-12	83
R^{P306}	ϕ	-94	-61	-147	31
	ψ	120	131	146	9
I^{P307}	ϕ	-97	-110	-118	8
	ψ	121	123	160	17
H^{P308}	ϕ	-91	-94	-129	16
	ψ	126	106	121	8
I^{P309}	ϕ	-87	-93	-84	3
	ψ	**-43**	**-27**	**140**	**82**
G^{P312}	ϕ	-149	-157	-158	4
	ψ	-169	-178	131	25
P^{P313}	ϕ	-70	-55	-59	6
	ψ	149	122	99	17
G^{P314}	ϕ	77	70	100	12
	ψ	**-136**	**8**	**8**	**96**
R^{P315}	ϕ	-73	-123	-172	33
	ψ	5	129	149	60
A^{P316}	ϕ	-82	-147	-131	25
	ψ	66	150	167	41
F^{P317}	ϕ	-147	-117	-133	10
	ψ	161	165	153	4
Y^{P318}	ϕ	-133	53	60	76
	ψ	151	41	65	44
T^{P319}	ϕ	-97	-80	-150	27
	ψ	156	4	-2	69
T^{P320}	ϕ	-141	-62	-101	26
	ψ			47	0

[a]The average deviation from the mean of the three torsion angles (from B4e8, 2219 and gp120)